SHEAR REINFORCEMENT IN DEEP SLABS

by

Stanley C. Woodson, PhD, PE

US Army Engineer Waterways Experiment Station

Vicksburg, Mississippi

INTRODUCTION

A considerable amount of data is available in the literature regarding the behavior of normally-proportional slabs. Woodson (1993) presented one of the most comprehensive collections of data on statically- and dynamically-tested slabs. The data base was used in the development of the Engineer Technical Letter (ETL) 1110-9-7, "Response Limits and Shear Design for Conventional Weapons Resistant Slabs," published by the U.S. Army Corps of Engineers in September, 1990. The ETL is the most recently published design document on the subject, and it claims no applicability to slabs having span-to-effective-depth (Lid) ratios less than 5. In addition, the ETL sets forth specific shear reinforcement requirements for laterally-restrained slabs with Lid values less than 8. Thus, guidance for shear design and response limits of deep slabs used in protective structures is lacking, particularly for structures to resist the effects of conventional weapons.

Thirteen one-way reinforced concrete slabs were statically loaded at the U.S. Army Engineer Waterways Experiment Station (WES) in March through April, 1993. The following sections describe the slabs' construction details, reaction structure, instrumentation, experimental procedure, material properties, and the experimental procedure.

Specimen Details

Previous studies (Woodson, 1993) emphasized that the primary parameters that affect the large-deflection behavior of a one-way slab include: support conditions, quantity and spacing of principal reinforcement, quantity and spacing of shear reinforcement, span-to-effective-depth (Lid) ratio, and scaled range (for blast loads). The slabs in this study were designed with consideration of the role of these primary parameters. Table 1 qualitatively presents the characteristics of each slab. Table 2 presents the same characteristics in a quantitative manner, reflecting the practical designs based on available construction materials. All slabs were

Report Documentation Page

Form Approved
OMB No. 0704-0188

1. REPORT DATE	2. REPORT TYPE	3. DATES COVERED
AUG 1994		**00-00-1994 to 00-00-1994**

4. TITLE AND SUBTITLE	5a. CONTRACT NUMBER
Shear Reinforcement in Deep Slabs	5b. GRANT NUMBER
	5c. PROGRAM ELEMENT NUMBER
6. AUTHOR(S)	5d. PROJECT NUMBER
	5e. TASK NUMBER
	5f. WORK UNIT NUMBER
7. PERFORMING ORGANIZATION NAME(S) AND ADDRESS(ES) **U.S. Army Engineer Waterways Experiment Station,3909 Halls Ferry Road,Vicksburg,MS,39180-6199**	8. PERFORMING ORGANIZATION REPORT NUMBER
9. SPONSORING/MONITORING AGENCY NAME(S) AND ADDRESS(ES)	10. SPONSOR/MONITOR'S ACRONYM(S)
	11. SPONSOR/MONITOR'S REPORT NUMBER(S)

12. DISTRIBUTION/AVAILABILITY STATEMENT
Approved for public release; distribution unlimited

13. SUPPLEMENTARY NOTES
See also ADM000767. Proceedings of the Twenty-Sixth DoD Explosives Safety Seminar Held in Miami, FL on 16-18 August 1994.

14. ABSTRACT

15. SUBJECT TERMS

16. SECURITY CLASSIFICATION OF:			17. LIMITATION OF ABSTRACT	18. NUMBER OF PAGES	19a. NAME OF RESPONSIBLE PERSON
a. REPORT **unclassified**	b. ABSTRACT **unclassified**	c. THIS PAGE **unclassified**	**Same as Report (SAR)**	**41**	

designed to be loaded in a clamped (laterally and rotationally restrained) condition. Each slab had a clear span of 24 inches and a width of 24 inches. Slab thickness 2

varied as follows: 3 slabs had an overall thickness of 5.5 inches, and 10 slabs had an overall thickness of 8.9 inches. The effective depth of each slab was either approximately 4.8 or 8.0 inches. The Lid ratio of each slab was either 3 or 5.

In general, the experimental program was designed to study the behavior of uniformly-loaded deep slabs, including a comparison of the effects of lacing bars and stirrups on the behavior. It was important that the ratio of principal steel spacing to slab effective depth (sld) was held nearly constant among the slabs. Data from previous studies indicated that this ratio should be less than 1.0 in order to enhance the large-deflection behavior. The s/d ratio was maintained at a value of approximately 0.5. Three shear reinforcement spacings were used: 0.17d, 0.31d, and 2d (d/2 is the value typically given in design manuals for blast-resistant structures). Figures 1 through 3 are plan views showing slab proportions and the principal steel and temperature steel layouts for each of the slabs. The temperature (transverse) steel spacing was identical for all of the slabs, but one difference in the temperature steel placement occurred between the laced and nonlaced slabs. The temperature steel is typically placed exterior to the principal steel in laced slabs, but it is placed interior to the principal steel in the slabs having stirrups or no shear reinforcement.

Figures 4 through 14 are sectional views cut through the lengths of the slabs. The dashed lacing bar in each figure indicates the configuration of the lacing bar associated with the next principal steel bar. The positions of the lacing bars were alternated to encompass all temperature steel bars. However, some temperature steel bars were not encompassed by lacing bars in slab no. 12 due to the spacing of the lacing bar bends. The spacings of the lacing bar bends were controlled by the shear reinforcement quantities in corresponding slabs with stirrups. In slabs with stirrups, the stirrups were spaced along the principal steel bar at the spacings shown in Table 2, never directly encompassing the temperature steel.

The slabs were constructed in the laboratory with much care to ensure quality construction with minimal error in reinforcement placement. For example, Figures 15 and 16 are photographs of slabs no. 1 and 2 prior to the placement of concrete.

Instrumentation

Each slab was instrumented for strain, displacement, and pressure measurements. The data were digitally recorded with a personal computer. Two displacement transducers were used in each experiment to measure vertical displacement of the slab, one at one-quarter span and one at midspan. The displacement transducers used were Coalesce Model PT-1 01, having a working range of 10 inches. These transducers measured the displacement of the slab by means of a potentiometer which detected the extension and retraction of a cable attached to a spring inside the transducer. More specifically, a Coalesce Model PT-101 transducer contains a drum that is attached to a linear rotary potentiometer. When the cable is completely

retracted, the potentiometer is at one end of its range. As the cable is extended, the drum rotates (thus rotating the potentiometer) until the cable is at full extension and the potentiometer is at the other end of its range. A DC voltage is applied across the potentiometer, and the output is taken from the potentiometer's wiper. As the cable is retracted and the wiper moves along the potentiometer, the output voltage varies since the potentiometer acts as a voltage divider. The body of each transducer was mounted to the floor

of the reaction structure, and the cable was attached to a hook that was glued to the slab surface. Retraction of the cables into the transducers' bodies occurred as the slab deflected and downward displacement occurred at the one-quarter span and midspan locations. Two single-axis, metal film, 0.125-inch-long, 350 ohm, strain gage pairs were installed on principal reinforcement in each slab. Each pair consisted of a strain gage on a top bar and one on a bottom bar directly below. One pair was located at midspan (ST-I, SB-1), and one was located at one-quarter span (ST-2, SB-2).

Strain gages were also installed at mid-height on shear steel in the slabs that contained shear reinforcement. Strain gages were placed on lacing bars in laced slabs at locations along the length of the slabs similar to the locations of stirrups with gages in the corresponding slabs with stirrups. The gages were placed on the shear reinforcement associated with the center principal steel bars. Two Kulite Model HKM-S375, 500-psi-range pressure gages (PI and P2) were mounted in the bonnet of the test chamber in order to measure the water pressure applied to the slab.

Experimental Procedure

The 64oot diameter blast load generator was used to slowly load the slabs with water pressure. Huff (1969) presented a detailed description of the test device. Preparations for the experiments began with the reaction structure being placed inside the test chamber and surrounded with compacted sand. In general, the reaction structure consisted of a steel/concrete box without a top. Bolts for clamping the slabs protruded upward from the two sides. The reaction structure had a removable door to allow access to the space beneath the slab specimen, particularly for instrumentation requirements. Placement of a 36- by 24-inch slab in the reaction structure allowed 6 inches of the slab at each end to be clamped by a steel plate that was bolted into position, thereby leaving a 24- by 24-inch one-way restrained slab to be loaded with uniform pressure. After a slab was placed on the reaction structure, the wire leads from the instrumentation gages and transducers were connected. After placing the removable door into position, the sand backfill was completed on the door side of the reaction structure. A 118-inch-thick fiber-reinforced neoprene rubber membrane and a 118-inch-thick unreinforced neoprene rubber membrane were placed over the slab, and 112- by 6- by 24-inch steel plates were bolted into position at each support. Prior to the bolting of the plates, a waterproofing puffy was placed between the membrane and the steel plates to seal gaps around the bolts in order to prevent a loss of water pressure during the experiment. The chamber's lid was lowered into position, and the chamber was rolled inside the large reaction

structure. A time of approximately 18 minutes was required to fill the bonnet indicated when the bonnet had been filled. At that time, the waterline valve was again closed to allow closing of the relief plug. The waterline valve was once again opened slowly, inducing a slowly increasing load to the slab's surface as the lid of the chamber was pushed upward and against the large reaction structure. A pump was connected to the waterline to facilitate water pressure loading in the case that commercial line pressure was not great enough to reach ultimate resistance of the slab in any of the experiments. Monitoring of the pressure gages and deflection gages indicated the behavior of the slab during the experiment and enabled this author to make decision for experiment termination. The loading was controlled at a slowly changing rate, resulting in a load application time of several minutes. Following experimentation termination, measurements and photographs of the slab were taken after removal of the neoprene membrane. Finally, the damaged slab was removed and the reaction structure was prepared for another slab.

Table 1 Slab Characteristics (Qualitative)

Table 1
Slab Characteristics (Qualitative)

Slab	$\rho_{tension}$	ρ_{shear}	Lacing	Stirrups	Principal Steel Spacing	Shear Steel Spacing	L/d Ratio
1	large	none	-	-	0.5d	-	5
2	large	large	-	x	0.5d	0.31d	5
3	large	large	x	-	0.5d	0.31d	5
4	small	none	-	-	0.5d	-	3
5	large	none	-	-	0.5d	-	3
6	large	none	-	-	0.5d	-	3
7	small	large	-	x	0.5d	0.17d	3
8	large	large	-	x	0.5d	0.17d	3
9	large	large	-	x	0.5d	0.17d	3
10	large	small	-	x	0.5d	2d	3
11	small	large	x	-	0.5d	0.17d	3
12	large	small	x	-	0.5d	2d	3
13	large	large	x	-	0.5d	0.17d	3

Table 2 Slab Characteristics (Qualitative)

Table 2
Slab Characteristics (Quantitative)

Slab	$\rho_{tension}$	ρ_{shear}	Lacing	Stirrups	Principal Steel Spacing (Inches)	Shear Steel Spacing (Inches)	L/d Ratio
1	0.0096	none	-	-	No. 3 @ 2.4	-	5
2	0.0096	0.0060	-	x	No. 3 @ 2.4	1.5	5
3	0.0096	0.0060	x	-	No. 3 @ 2.4	1.5	5
4	0.0034	none	-	-	No. 3 @ 4.0	-	3
5	0.0096	none	-	-	No. 3 @ 4.0	-	3
6	0.0096	none	-	-	No. 3 @ 4.0	-	3
7	0.0034	0.0060	-	x	No. 3 @ 4.0	1.33	3
8	0.0096	0.0060	-	x	No. 3 @ 4.0	1.33	3
9	0.0096	0.0060	-	x	No. 3 @ 4.0	1.33	3
10	0.0096	0.0013	-	x	No. 3 @ 4.0	6.00	3
11	0.0034	0.0060	x	-	No. 3 @ 4.0	1.33	3
12	0.0096	0.0013	x	-	No. 3 @ 4.0	6.00	3
13	0.0096	0.0060	x	-	No. 3 @ 4.0	1.33	3

RESULTS AND DISCUSSION

General

In general, the quality of the data was good. Data were recovered from all gages, and it appears that all gages functioned properly.

Posttest measurements and inspection provided a data check and damage assessment of each slab prior to removal from the reaction structure. Indicating the types of damage incurred in the series, Figures 17 through 20 show the posttest condition of four of the slabs (slabs no. 1, 2, 7, and 13).

Discussion

Figure 21 shows the general shape of the midspan load-deflection curve. Values of load and deflection at points A through C of Figure 21 are given in Table 3 for convenience in numerical comparisons. Similarly, Table 4 presents load-deflection values recorded at the quarter-span location for each slab.

Figures 22 through 28 present composite graphs of the load-deflection curves of the slabs. Figure 22 demonstrates the significance of shear reinforcement (see Table 1) in that slab no. 1 was not able to achieve the value of ultimate resistance for slabs no. 2 and 3. Lacing bars and stirrups apparently provided approximately the same level of contribution to the shear strength of the slabs.

Figure 23 simply indicates the differences in strength due to the Lid values. Figure 24 shows that the replication associated with slabs no. 5 and 6 provided very similar results.

Figure 25 compares the effects of stirrups, lacing, and no shear reinforcement of the slabs with an Lid of 3. As was shown in Figure 22 for the slabs with an Lid of 5, shear reinforcement did make a significant contribution to the ultimate resistance and lacing and stirrups were of approximately equal effectiveness. Figure 26 indicates that the data are consistent in that the smaller amount of shear reinforcement (slab no. 10) was less effective than the larger amount. In all Figures containing slab no. 10, the data shown past the ultimate resistance for slab no. 10 is not true data since the deflection transducer cable apparently broke loose from the slab shortly after the ultimate resistance was reached.

Figure 27 further supports the previous observation that the lacing bars and stirrups are similarly effective in enhancing ultimate shear resistance. However, this data indicates that stirrups may be slightly more effective at these steel ratios. Figure 28 further supports the considerable difference in effectiveness for large and small quantities of shear reinforcement.

Two commonly-used parameters for describing slab response are the midspan-deflection-to-thickness ratio and the equivalent support rotation (defined as the arctan of the quotient of the midspan deflection divided by one-half of the clear span). Actually, for predominantly shear response, as is generally the case for deep slabs, neither of these parameters fully describe the response. However, attempts should be made to correlate the allowable response of deep slabs with these parameters for consistency in guidance documents.

Tables 5 and 6 respectively present the midspan-deflection-to-thickness ratios and the equivalent support rotations for each slab at intervals corresponding to points A, B, and C of Figure 21. Table 5 shows that the midspan-deflection-to-slab-thickness ratio at ultimate
(δ_A/t) is considerably small for deep slabs. For normally-proportioned slabs, this ratio has the general value of 0.3 to 0.5.

The values given in Table 6 are useful in that they provide information to the designer as to what equivalent support rotation should ultimate resistance be expected to occur. Additionally, Table 6 shows that deep slabs can achieve considerably high values of response without collapse. Values of equivalent support rotation up to approximately 16 degrees were sustained.

From an analytical/design viewpoint, Table 7 demonstrates the application of compression membrane theory (Park and Gamble, 1980). The W_y values in Table 7 correspond to yield-line theory, and the W_c values correspond to compression membrane theory. The W_c values were computed using the **(δ_A/t)** values supplied in Table 5. For most of the slabs that contained a "large" amount of shear reinforcement, the experimental values and the W_c values compare rather well. Slabs with no or little shear reinforcement incurred shear failures prior to attaining the compressive membrane resistance values.

CONCLUSIONS

A relatively large amount of shear reinforcement is critical for achieving the potential ultimate resistance of a deep slab. The post-ultimate behavior of the slabs presented indicates that a substantial amount of

reserve capacity is available in deep slabs.

Compression membrane theory provides a good estimate of the potential ultimate resistance of a deep slab, provided appropriate values of **(δ_A/t)** are used in the computations. The **(δ_A/t)** values were approximately 0.07 and 0.03 to 0.05 for the slabs with Lid values of 5 and 3, respectively. Since, these **(δ_A/t)** values resulted in slightly high compressive membrane resistance values, **(δ_A/t)** should be increased slightly in order to decrease the W_c values and to provide conservative design values.

Table 3 Midspan Load-Deflection Summary

Table 3
Midspan Load-Deflection Summary

Slab	P_A (psi)	δ_A	P_B (psi)	δ_B	P_C (psi)	δ_C
1	399	0.20	264	1.01	349	1.98
2	571	0.40	396	0.96	369	1.80
3	543	0.41	319	1.32	-	-
4	572	0.33	-	-	-	-
5	1169	0.24	869	1.30	1211	1.92
6	1222	0.33	824	1.43	1150	2.66
7	1860	0.40	-	-	-	-
8	1550	0.40	975	1.74	1225	2.58
9	1365	0.29	1285	0.44	1260	0.87
10	1337	0.29	-	-	-	-
11	1380	0.37	-	-	-	-
12	1210	0.27	926	1.21	1163	2.93
13	1545	0.65	1315	1.79	1445	3.48

Table 4 Quarter-span Load-Deflection Summary

Table 4 Quarter-span Load-Deflection Summary						
Slab	P_A (psi)	δ_A	P_B (psi)	δ_B	P_C (psi)	δ_C
1	399	0.20	264	1.03	349	1.86
2	571	0.36	396	0.96	-	-
3	543	0.31	319	0.81	-	-
4	572	0.23	-	-	-	-
5	1169	0.23	869	1.30	1211	2.66
6	1222	0.28	824	1.48	1150	2.73
7	1860	0.32	-	-	-	-
8	1550	0.37	975	1.86	1225	2.58
9	1365	0.24	1285	0.46	1260	0.87
10	1337	0.29	-	-	-	-
11	1380	0.32	-	-	-	-
12	1210	0.27	926	1.32	1163	2.93
13	1545	0.53	1330	1.62	1445	3.48

Table 5 Midspan Deflection/Slab Thickness

Table 5 Midspan Deflection/Slab Thickness			
Slab	δ_A/t	δ_B/t	δ_C/t
1	0.04	0.18	0.36
2	0.07	0.17	0.33
3	0.07	0.24	-
4	0.04	-	-
5	0.03	0.15	0.35
6	0.04	0.16	0.30
7	0.05	-	-
8	0.05	0.20	0.29
9	0.03	0.05	0.16
10	0.03	-	-
11	0.04	-	-
12	0.03	0.14	0.33
13	0.04	0.20	0.39

Table 6 Equivalent Support Rotation

Table 6 Equivalent Support Rotation				
Slab	L/d	θ_A (degrees)	θ_B (degrees)	θ_C (degrees)
1	5	1.0	4.8	9.4
2	5	1.9	4.6	8.5
3	5	2.0	6.3	-
4	3	1.6	-	-
5	3	1.1	6.2	9.1
6	3	1.6	6.8	12.5
7	3	1.9	-	-
8	3	1.9	8.3	12.1
9	3	1.4	2.1	4.1
10	3	1.4	-	-
11	3	1.8	-	-
12	3	1.3	5.8	13.7
13	3	3.1	8.5	16.2

Table 7 Compressive Membrane

Table 7 Compressive Membrane					
Slab	W_y (psi)	W_c (psi)	Experimental (psi)	ρ_{shear}	$\frac{\delta_A}{t}$ (experimental)
1	348	606	399	0	0.036
2	348	595	571	0.0060	0.073
3	348	594	543	0.0060	0.075
4	352	1331	572	0	0.037
5	966	1718	1169	0	0.027
6	966	1713	1222	0	0.037
7	352	1322	1860	0.0060	0.045
8	966	1705	1550	0.0060	0.045
9	966	1716	1365	0.0060	0.033
10	966	1716	1337	0.0013	0.033
11	352	1326	1380	0.0060	0.042
12	966	1717	1210	0.0013	0.030
13	966	1668	1545	0.0060	0.073

References

Woodson, S.C., "Effects of Shear Reinforcement on the Large-Deflection Behavior of Reinforced Concrete Slabs," thesis, University of Illinois at Urbana-Champaign, 1993.

Park, R., and Gamble, W.L., Reinforced Concrete Slabs, John Wiley and Sons, New York, pp. 562-609,1980.

Huff, W.L., "Test Devices of the Blast Load Generator Facility," Miscellaneous Paper N-69-1, U.S. Army Engineer Waterways Experiment Station, Vicksburg, Mississippi, April 1969.

Figure 1- Plan View of slabs No. 1, 2, and 3

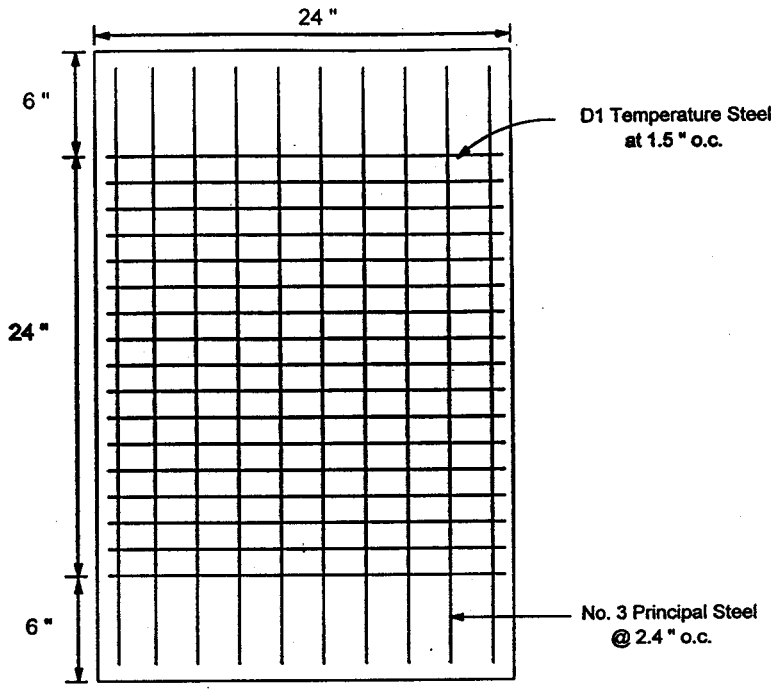

Figure 1. Plan View of Slabs No. 1, 2, and 3

Figure 2. Plan View of Slabs No. 4, 5, 6, 7, 8, 9, 111 and 13

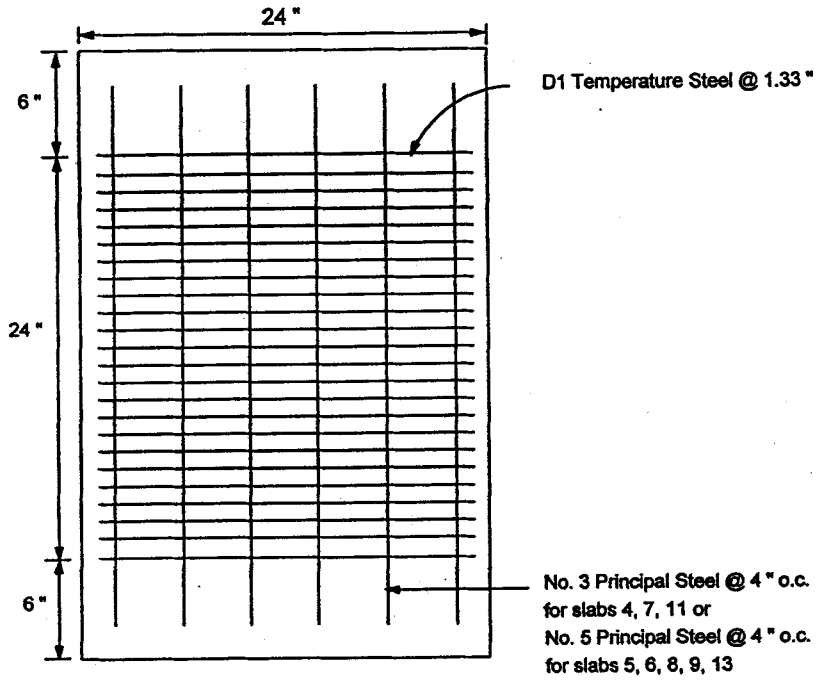

Figure 2. Plan View of Slabs No. 4, 5, 6, 7, 8, 9, 11, and 13

Figure 3. Plan View of Slabs No. 10 and 12

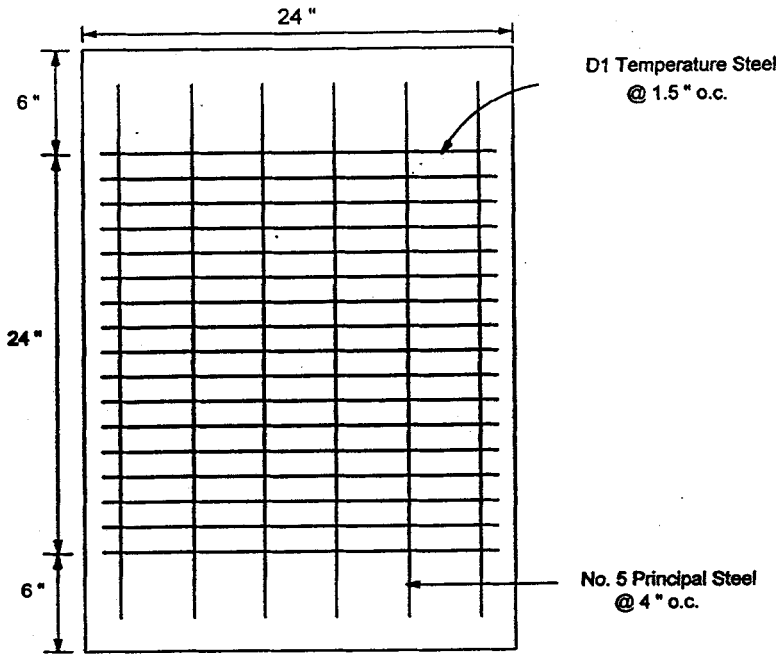

Figure 3. Plan View of Slabs No. 10 and 12

Figure 4. Sectional View Through Length of Slab No. 1

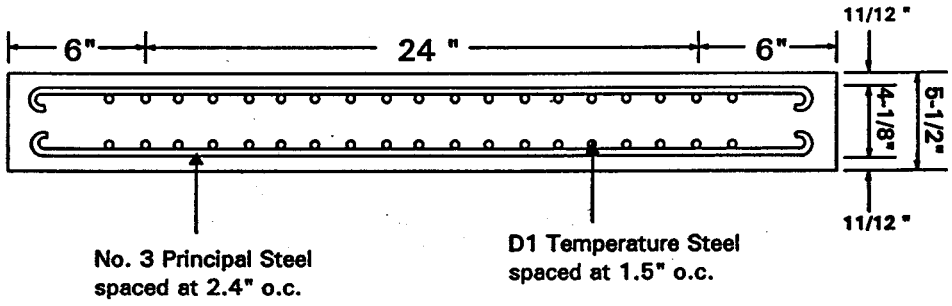

Figure 4. Sectional View Through Length of Slab No. 1

Figure 5. Sectional View Through Length of Slab No. 2

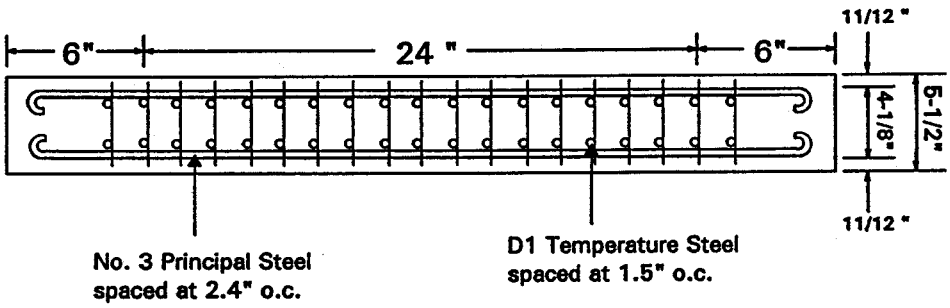

Figure 5. Sectional View Through Length of Slab No. 2

Figure 6. Sectional View Through Length of Slab No. 3

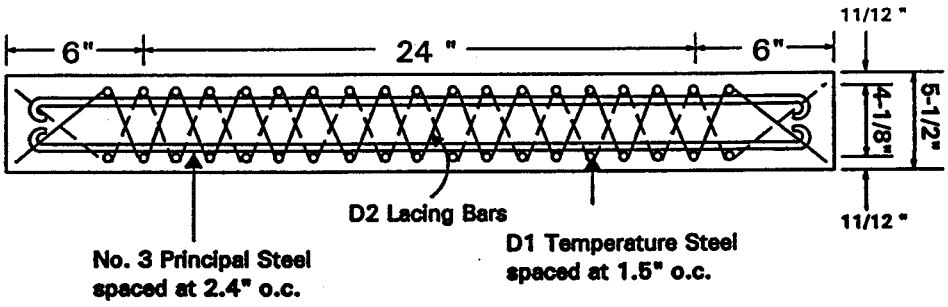

Figure 6. Sectional View Through Length of Slab No. 3

Figure 7. Sectional View Through Length of Slab No. 4

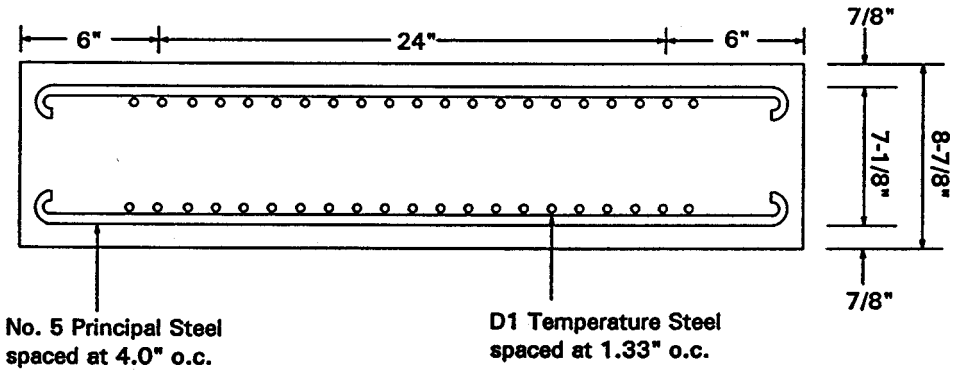

Figure 7. Sectional View Through Length of Slab No. 4

Figure 8. Sectional View Through Length of Slabs No. 5 & 6

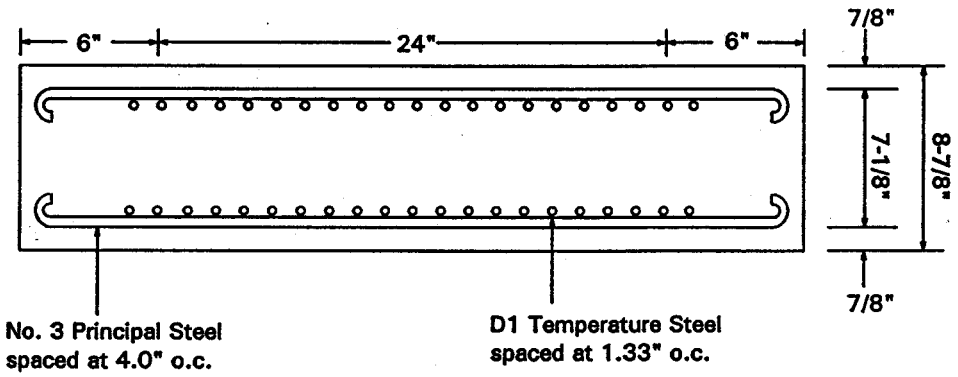

Figure 8. Sectional View Through Length of Slabs No. 5 & 6

Figure 9. sectional View Through Length of Slab No. 7

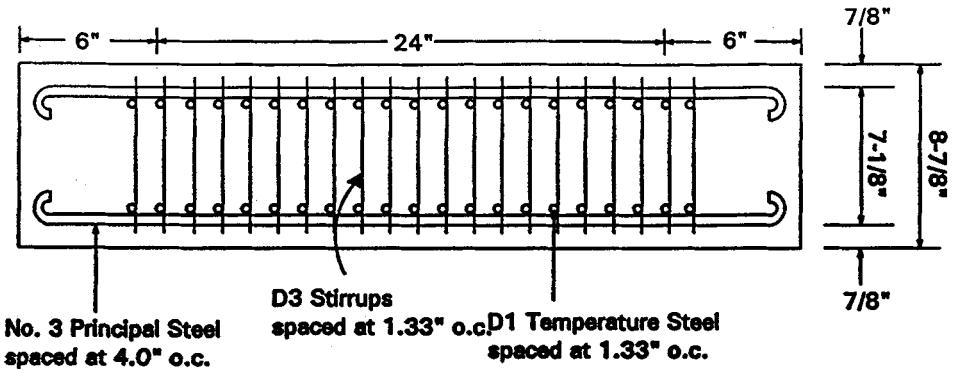

Figure 9. Sectional View Through Length of Slab No. 7

Figure 10. sectional View Through Length-of Slabs No. 8 & 9

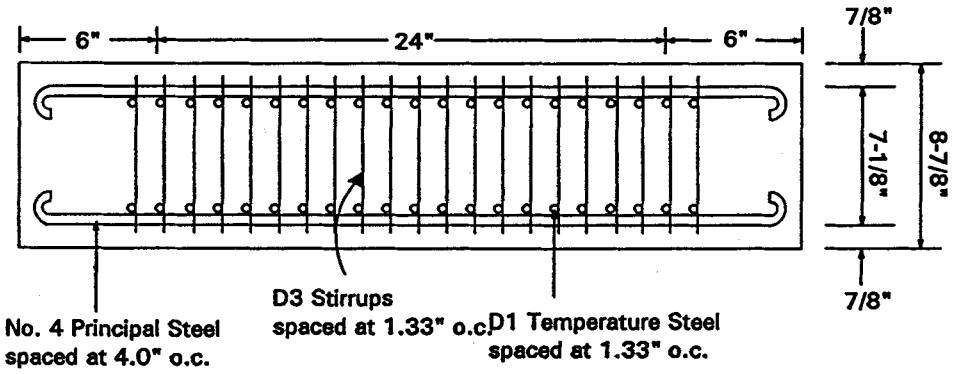

Figure 10. Sectional View Through Length of Slabs No. 8 & 9

Figure 11. Sectional View Through Length of Slab No. 10

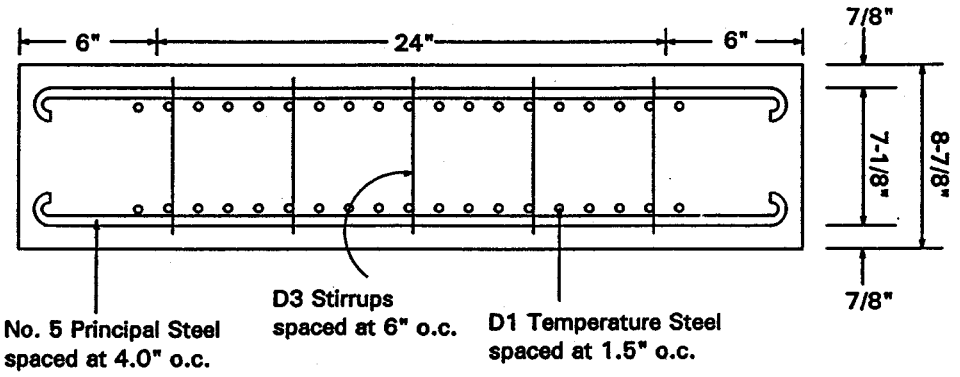

Figure 11. Sectional View Through Length of Slab No. 10

Figure 12. Sectional View Through Length of Slab No. 11

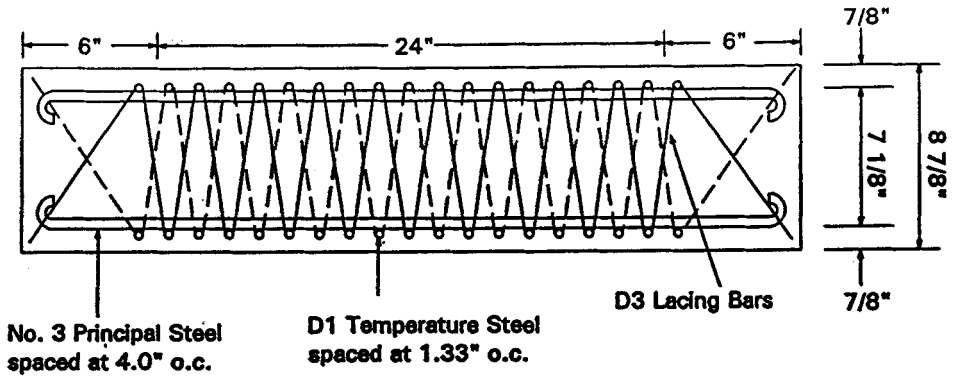

Figure 12. Sectional View Through Length of Slab No. 11

Figure 13. Sectional View Through Length of Slab No. 12

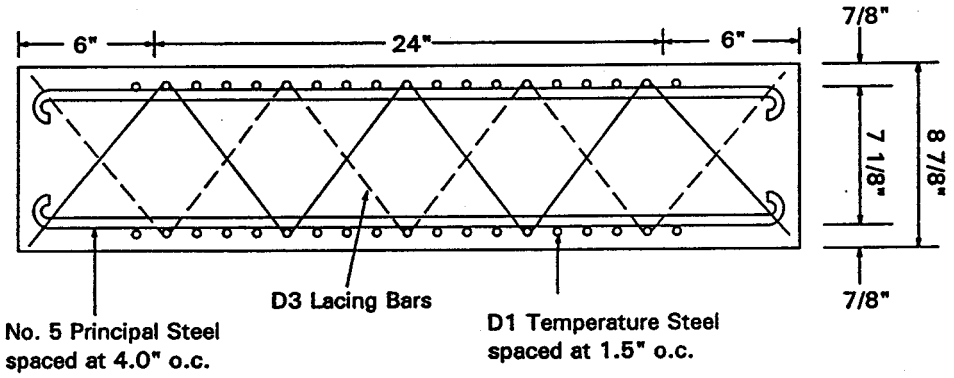

Figure 13. Sectional View Through Length of Slab No. 12

Figure 14. Sectional View Through Length of Slab No. 13

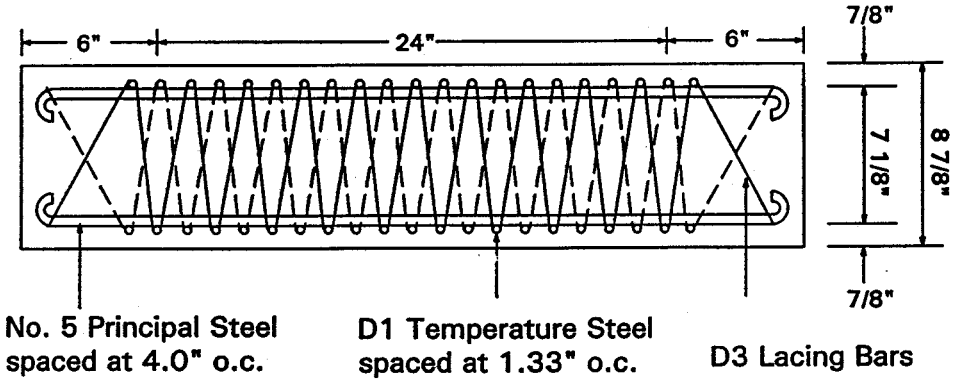

Figure 14. Sectional View Through Length of Slab No. 13

Figure 15. Slab No. 1 Prior to Concrete Placement

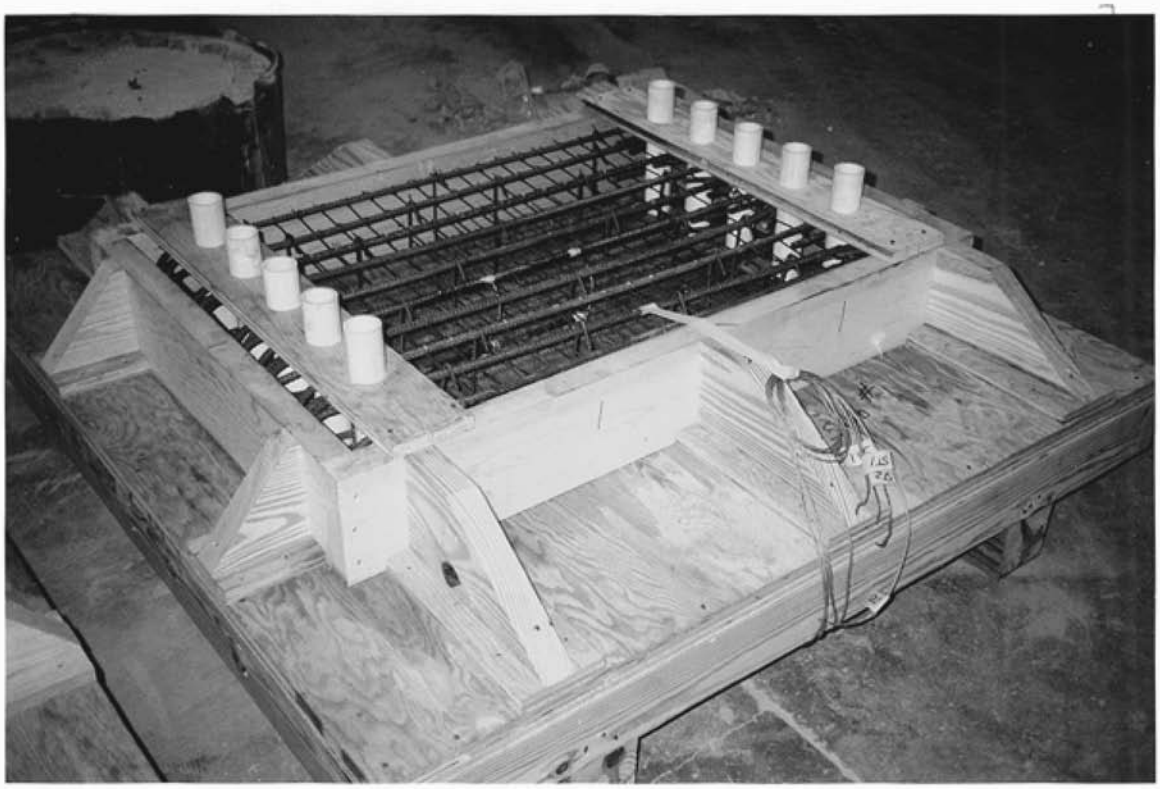

Figure 15. Slab No. 1 Prior to Concrete Placement

Figure 16. Slab No. 2 Prior to Concrete Placement

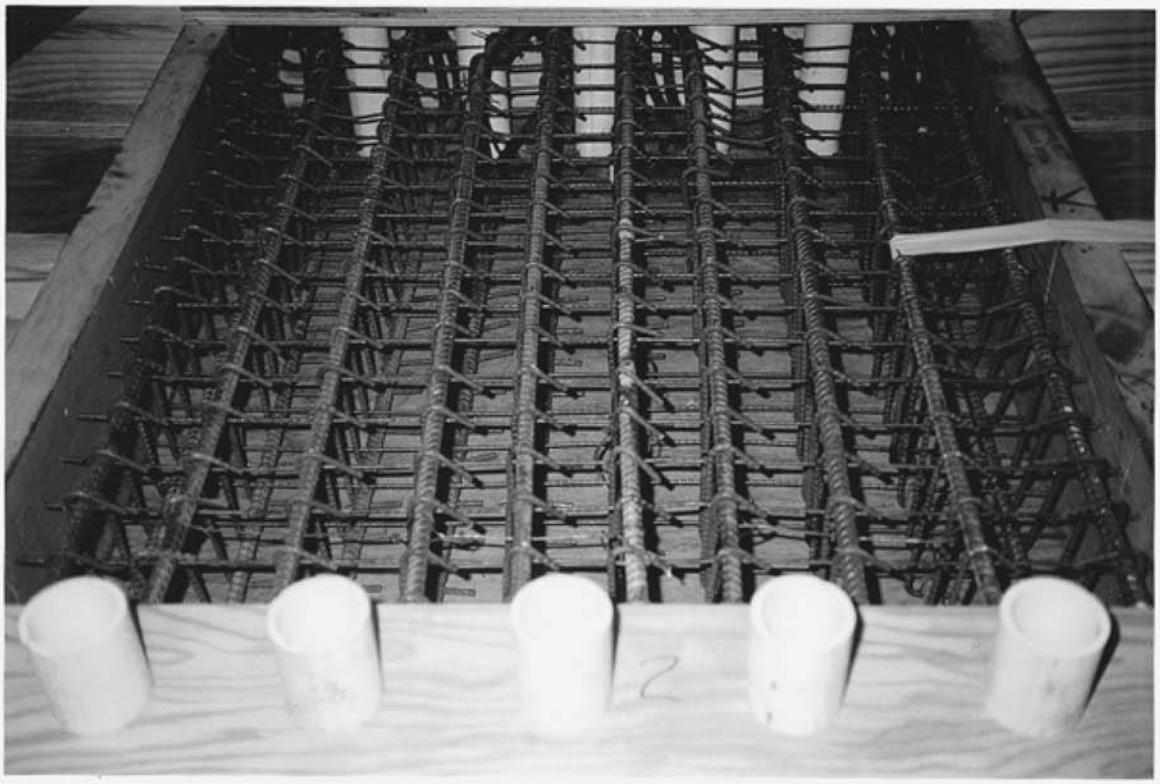

Figure 16. Slab No. 2 Prior to Concrete Placement

Figure 17. Posttest View of Slab No. 1

Figure 17. Posttest View of Slab No. 1

Figure 18. Posttest View of Slab No. 2

Figure 18. Posttest View of Slab No. 2

Figure 19. Posttest View of Slab No. 7

Figure 19. Posttest View of Slab No. 7

Figure 20. Posttest View of Slab No. 13

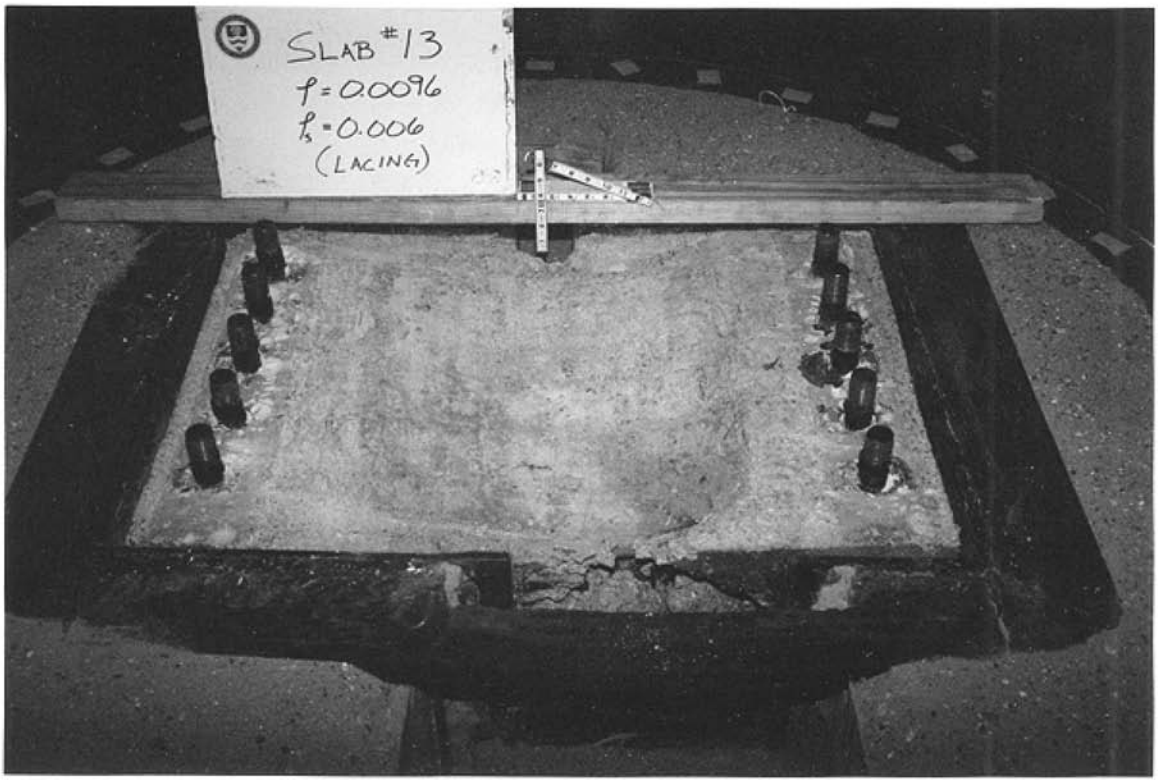

Figure 20. Posttest View of Slab No. 13

Figure 21. General Load-Deflection Curve

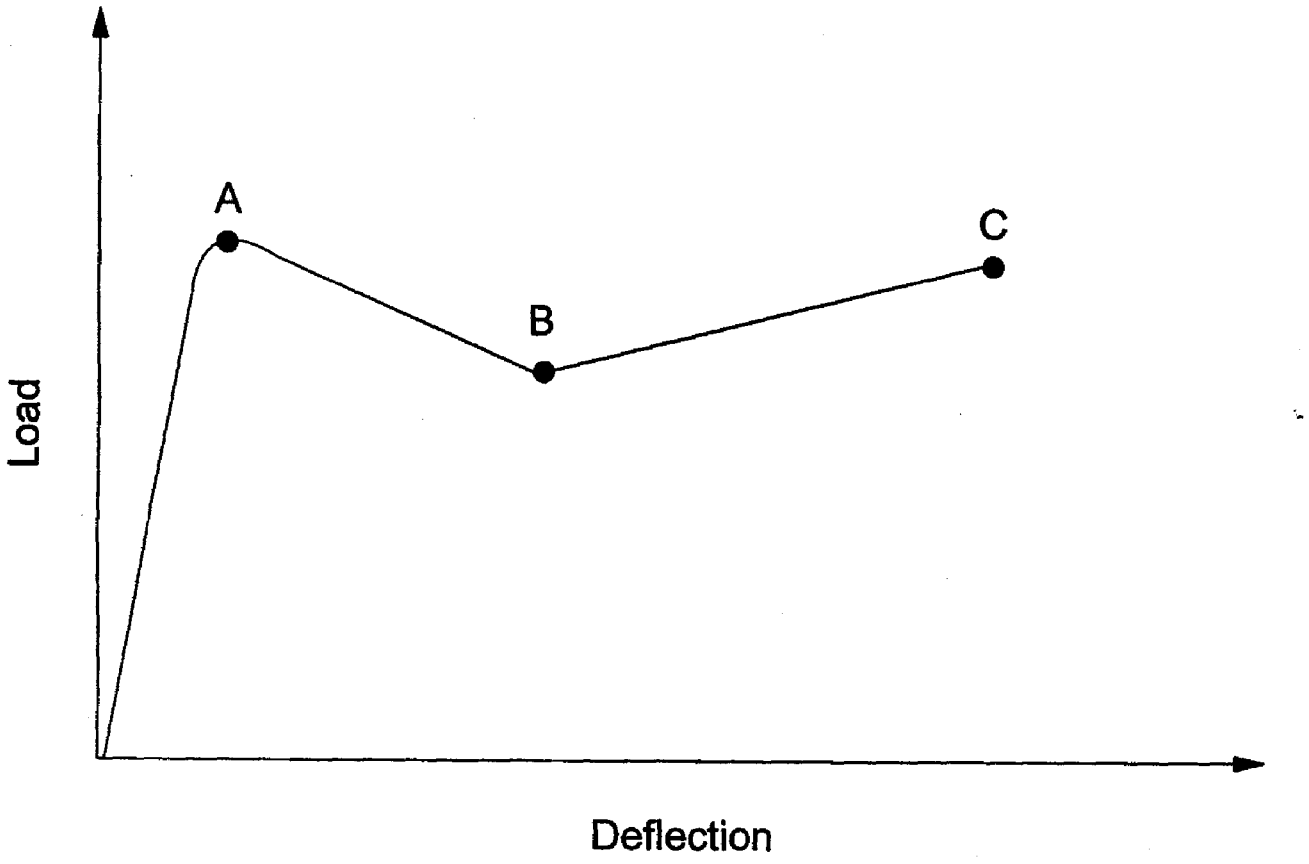

Figure 21. General Load-Deflection Curve

Figure 22. Composite Midspan Load-Deflection Data for Slabs No. 1, 2, and 3

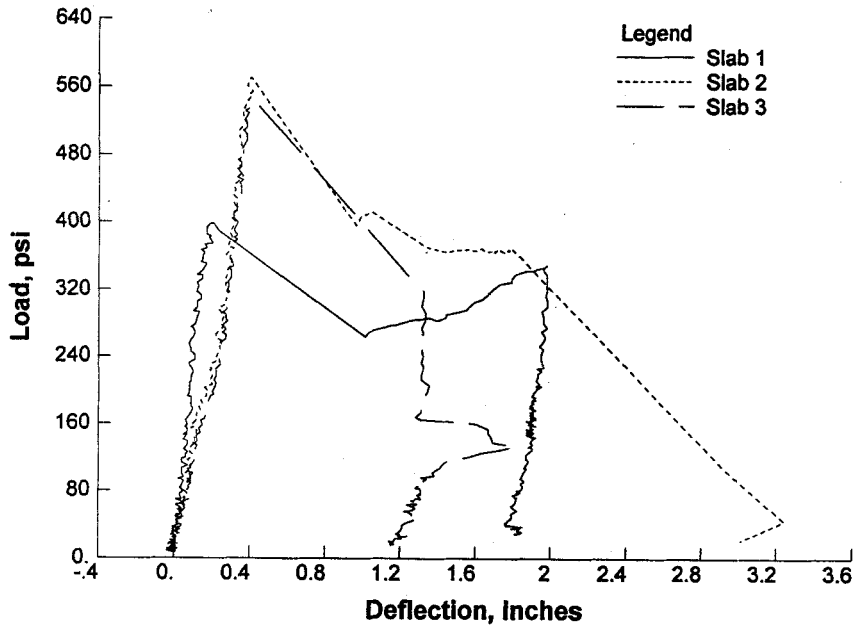

Figure 22. Composite Midspan Load-Deflection Data for Slabs No. 1, 2, and 3

Figure 23. Composite Midspan Load-Deflection Data for Slabs No. 1 and 5

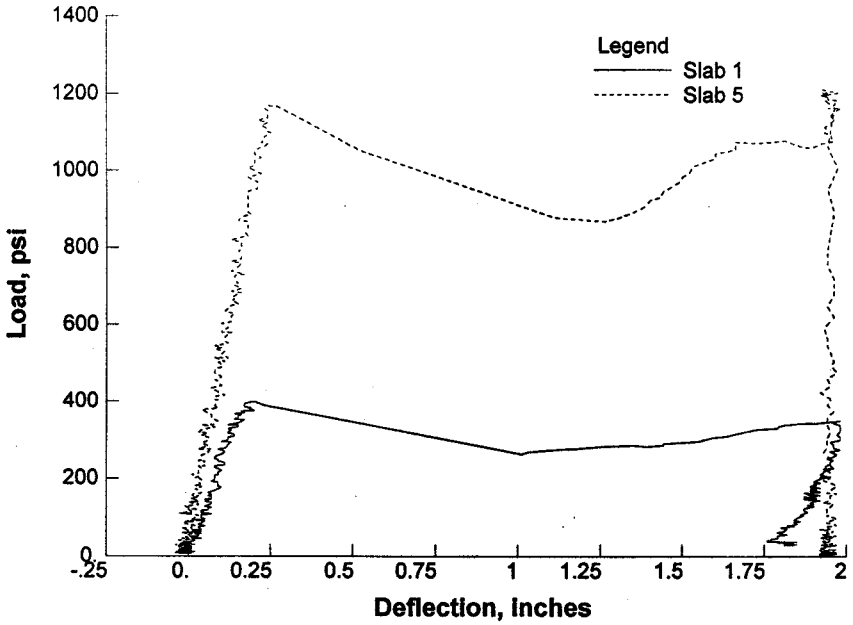

Figure 23. Composite Midspan Load-Deflection Data for Slabs No. 1 and 5

Figure 24. Composite Midspan Load-Deflection Data for Slabs No. 5 and 6

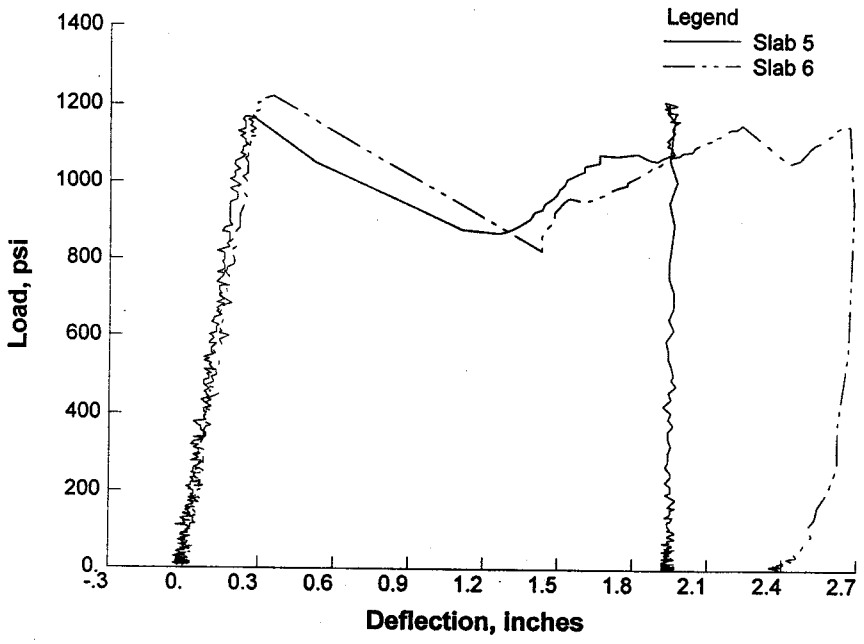

Figure 24. Composite Midspan Load-Deflection Data for Slabs No. 5 and 6

Figure 25. Composite Midspan Load-Deflection Data for Slabs No. 6, 8, and 13

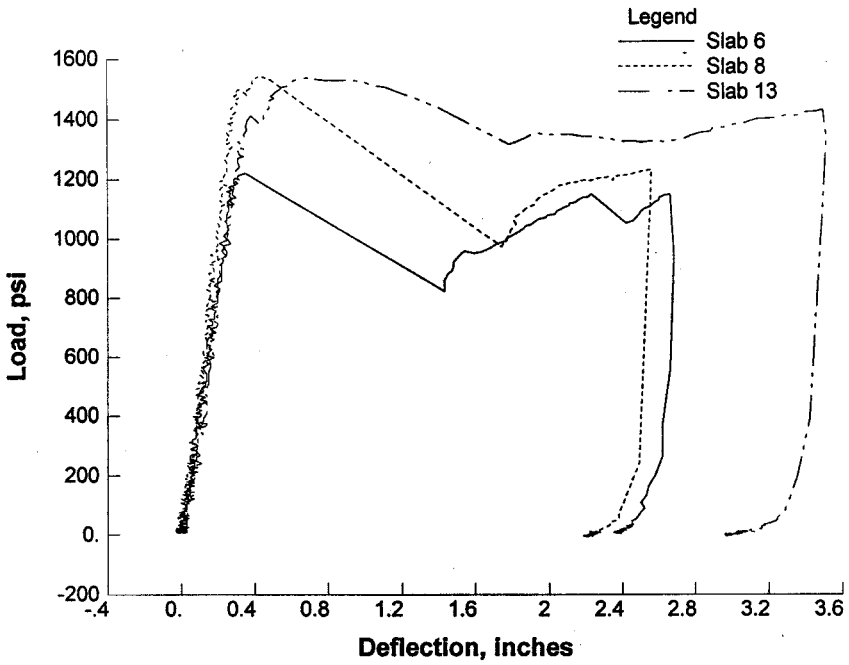

Figure 25. Composite Midspan Load-Deflection Data for Slabs No. 6, 8, and 13

Figure 26. Composite Midspan Load-Deflection Data for Slabs No. 8 and 10

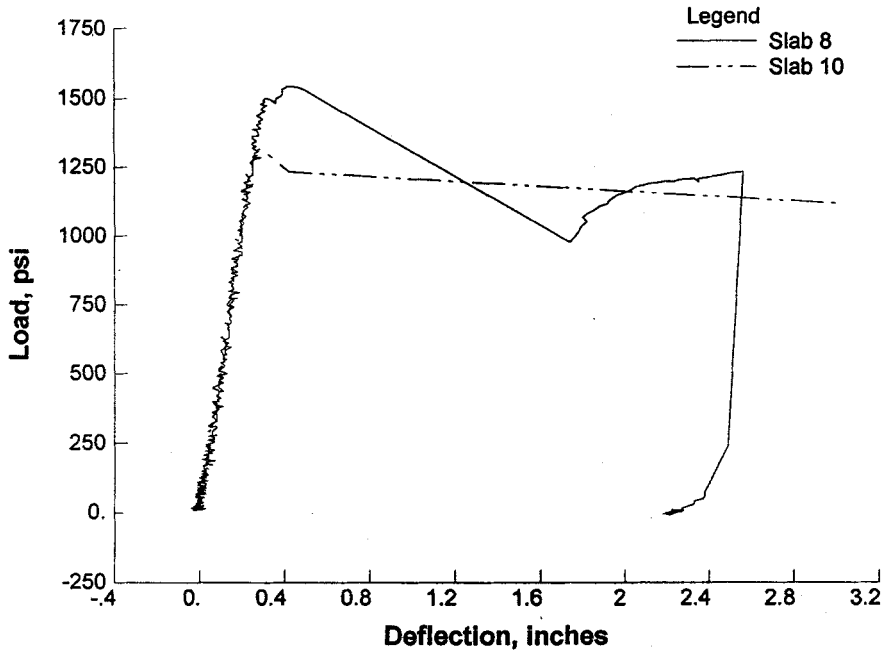

Figure 26. Composite Midspan Load-Deflection Data for Slabs No. 8 and 10

Figure 27. Composite Midspan Load-Deflection Data for Slabs No. 12 and 10

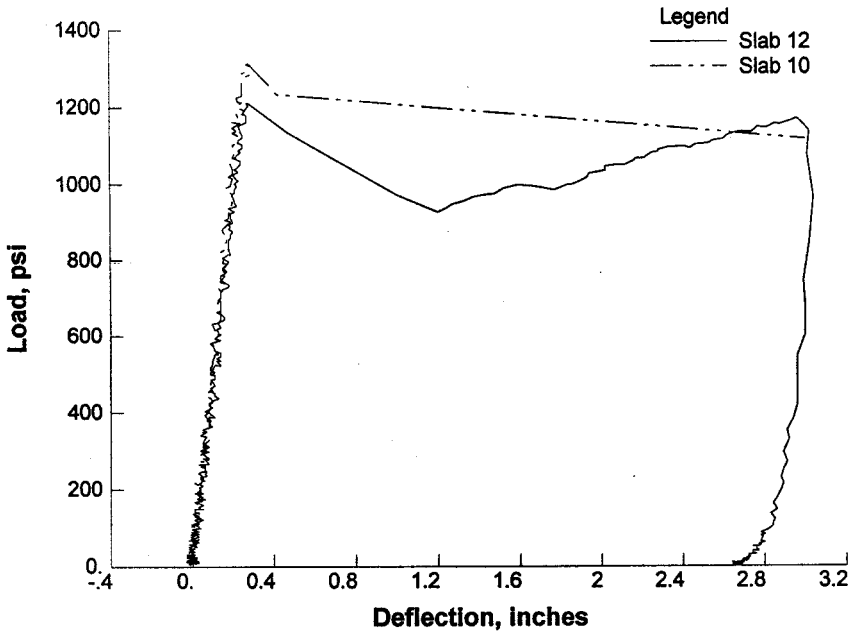

Figure 27. Composite Midspan Load-Deflection Data for Slabs No. 12 and 10

Figure 28. Composite Midspan Load-Deflection Data for Slabs No. 12 and 13

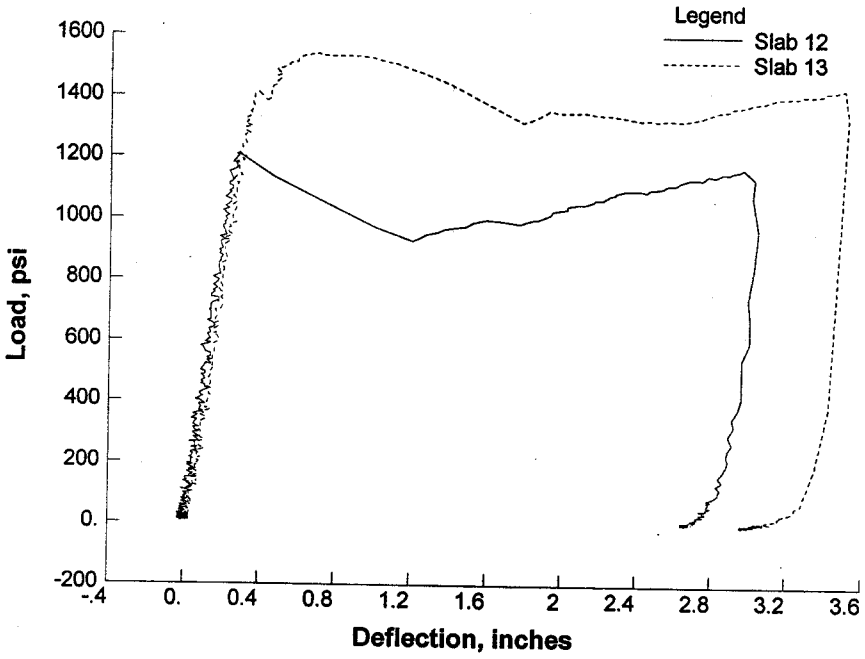

Figure 28. Composite Midspan Load-Deflection Data for Slabs No. 12 and 13